Carderock Division, Naval Surface Warfare Center

Bethesda, Maryland 20084-5000

CRDKNSWC/HD-0011-25 May 1997

Hydromechanics Directorate
Research and Development Report

BODY FORCES FOR AN FF1052 PROPELLER

BY

CAROL L. TSENG
PHUC NGUYEN
AND
DONALD FUHS

19970618 093

MAJOR CARDEROCK DIVISION TECHNICAL COMPONENTS

CODE 011   Director of Technology

10   Machinery Systems/Programs and Logistics Directorate

20   Ship Systems and Programs Directorate

50   Hydromechanics Directorate

60   Survivability, Structures and Materials Directorate

70   Signatures Directorate

80   Machinery Research and Development Directorate

90   Machinery In-Service Engineering Directorate

CARDEROCK DIVISION, NSWC, ISSUES THREE TYPES OF REPORTS:

1. **CARDEROCKDIV reports, a formal series,** contain information of permanent technical value. They carry a consecutive numerical identification regardless of their classification or the originating directorate.

2. **Directorate reports, a semiformal series,** contain information of a preliminary, temporary, or proprietary nature or of limited interest or significance. They carry an alphanumerical identification issued by the originating directorate.

3. **Technical memoranda, an informal series,** contain technical documentation of limited use and interest. They are primarily working papers intended for internal use. They carry an identifying number which indicates their type and the numerical code of the originating directorate. Any distribution outside CARDEROCKDIV must be approved by the head of the originating directorate on a case-by-case basis.

REPORT DOCUMENTATION PAGE

Public reporting burden for this collection of information is estimated to average 1 hour per response, including the time for reviewing instructions, searching existing data sources, gathering and maintaining the data needed, and completing and reviewing the collection of information. Send comments regarding this burden estimate or any other aspect of this collection of information, including suggestions for reducing this burden, to Washington Headquarters Services, Directorate for Information Operations and Reports, 1215 Jefferson Davis Highway, Suite 1204, Arlington, VA 22202-4302, and to the Office of Management and Budget, Paperwork Reduction Project (0704-0188), Washington, DC 20503.

1. AGENCY USE ONLY (Leave blank)	2. REPORT DATE	3. REPORT TYPE AND DATES COVERED
	May 1997	Research and Development, Oct 95 to Sept 96

4. TITLE AND SUBTITLE	5. FUNDING NUMBERS
Body Forces for an FF1052 Propeller	

6. AUTHOR(S)

Carol L. Tseng, Phuc Nguyen and Donald Fuhs

7. PERFORMING ORGANIZATION NAME(S) AND ADDRESS(ES)	8. PERFORMING ORGANIZATION REPORT NUMBER
Hydromechanics Directorate, Code 5400 Carderock Division Naval Surface Warfare Center 9500 MacArthur Boulevard West Bethesda, MD 20817-5700	CRDKNSWC/HD-0011-25

9. SPONSORING / MONITORING AGENCY NAME(S) AND ADDRESS(ES)	10. SPONSORING / MONITORING AGENCY REPORT NUMBER
Office of Naval Research Mechanics and Energy Conversion S&T Division 333 800 N. Quincy Street Arlington, VA 22217	

11. SUPPLEMENTARY NOTES

12a. DISTRIBUTION / AVAILABILITY STATEMENT	12b. DISTRIBUTION CODE
Approved for public release; distribution is unlimited.	

13. ABSTRACT (Maximum 200 words)

This project is the beginning of an effort to develop a general method for computing the effect of the propeller on the flow around the stern of surface ships, by treating the propeller as a body force when using a Reynolds Averaged Navier-Stokes RANS code to compute the hull flow. The body force is a time average value that varies in the circumferential and radial directions across the propeller disk. An algorithm is shown for iterating between the propeller force calculation and the RANS wake calculation. The propeller force is computed using an unsteady lifting surface code PUF-2.1 developed by the Massachusetts Institute of Technology, and a RANS calculated nominal wake was provided by the University of Iowa. The test case is the FF1052 Fleet propeller. PUF-2.1 calculations were compared to measurements for both open water and behind hull using the RANS calculated wake. The sensitivity of the calculated forces to grid size and other input parameters was determined. The variation in unsteady loading on the blades is shown.

14. SUBJECT TERMS			15. NUMBER OF PAGES
			15
			16. PRICE CODE

17. SECURITY CLASSIFICATION OF REPORT	18. SECURITY CLASSIFICATION OF THIS PAGE	19. SECURITY CLASSIFICATION OF ABSTRACT	20. LIMITATION OF ABSTRACT
UNCLASSIFIED	UNCLASSIFIED	UNCLASSIFIED	

CONTENTS

FIGURES

TABLES

NOTATION

BF	Blade Frequency
c	Chord length
C_D	Blade section drag coefficient
C_F	Skin friction coefficient from ATTC formulation
D_p	Tip diameter
$\bar{e}_x$	Unit vector in axial direction
$\bar{e}_\theta$	Unit vector in circumferential direction
f	Maximum section camber
f_x	Axial pressure jump across blade
$\bar{f}_x$	Time average thrust on element of force disk
f_θ	Tangential pressure jump across blade
$\bar{f}_\theta$	Time average tangential force on element of force disk
J	Advance coefficient based on speed of advance, V_A/nD_P
K_Q	Torque coefficient, $Q/\rho n^2 D_p^5$
$K_Q(\theta_p)$	Torque on one blade when the blade generator line is at angle θ_p, nondimensionalized as the torque coefficient
$\overline{K}_Q(\theta)$	Time average torque acting on force disk elements at angle θ, nondimensionalized as the torque coefficient
K_T	Thrust coefficient, $T/\rho n^2 D_p^4$
$K_T(\theta_p)$	Thrust on one blade when the blade generator line is at angle θ_p, nondimensionalized as the thrust coefficient
$\overline{K}_T(\theta)$	Time average thrust acting on force disk elements at angle θ, nondimensionalized as the thrust coefficient
K_{Td}	Instantaneous value of thrust on a force disk element, nondimensionalized as the thrust coefficient
N	Number of propeller blades
n	Shaft speed, revolutions per second
$\bar{n}$	Unit vector normal to blade camber surface
P	Pitch of blade
Q	Torque
r	Radius
r_h	Hub radius
R_p	Tip radius
t	Maximum section thickness, or time
T	Thrust

V	Ship speed
V_A	Volume mean speed of advance
V_R	Radial velocity
V_T	Tangential velocity
V_X	Axial velocity
β	Advance angle
β_{nw}	Pitch angle of tip vortex in near wake (transition wake)
β_{uw}	Pitch angle of tip vortex in ultimate wake
Δp	Pressure jump across blade
ϕ	Pitch angle of blade at tip
Γ	Circulation about one blade
θ	Angle from top dead center
θ_p	Angle of blade generator line, $\theta_p = 2\pi n t$
ρ	Mass density of water
ξ	Angle relative to generator line, $\xi = \theta - \theta_p$
ξ_{LE}	Angle of leading edge relative to generator line
ξ_{TE}	Angle of trailing edge relative to generator line

ABSTRACT

This project is the beginning of an effort to develop a general method for computing the effect of the propeller on the flow around the stern of surface ships, by treating the propeller as a body force when using a Reynolds Averaged Navier-Stokes RANS code to compute the hull flow. The body force is a time average value that varies in the circumferential and radial directions across the propeller disk. An algorithm is shown for iterating between the propeller force calculation and the RANS wake calculation. The propeller force is computed using an unsteady lifting surface code PUF-2.1 developed by the Massachusetts Institute of Technology, and a RANS calculated nominal wake was provided by the University of Iowa. The test case is the FF1052 Fleet propeller. PUF-2.1 calculations were compared to measurements for both open water and behind hull using the RANS calculated wake. The sensitivity of the calculated forces to grid size and other input parameters was determined. The variation in unsteady loading on the blades is shown.

ADMINISTRATIVE INFORMATION

OBJECTIVES

The original objective of this project was to calculate the effect of the propeller on the flow around the stern of the FF1052. The scope of the project was subsequently expanded to include the development of a general method to compute propeller body forces for use with RANS calculations of the hull flow.

BACKGROUND

Stern and Toda [1,2] have performed Reynolds Averaged Navier-Stokes RANS calculations for a Series 60 ship hull by representing the propeller by a distribution of nonrotating body forces. The use of body forces reduces execution time and array sizes by eliminating the need to grid the rotating propeller at each time step. The propeller body forces are time-average forces that vary radially and circumferentially within the propeller disk. The strengths of the body forces were calculated using the Massachusetts Institute of Technology

1

MIT unsteady force program PUF-2 [3] and field point velocity calculations. The unsteady effective wake input to PUF-2 was computed by subtracting estimates of the propeller-induced velocities from the total velocities calculated by the RANS code. The estimates of induced velocities were confirmed by field point velocity calculations done using the circulation from PUF-2. It was necessary to iterate because the effective wake input to PUF-2 and field point velocity calculations depends on the output induced velocities, and the body forces input to the RANS code depend on the output total velocity. For the calculations of Stern et al [1], one pass through PUF-2 and the field point velocity program were made for each pass through the RANS code.

APPROACH

The approach used for the present FF1052 calculations is based on Stern and Toda's previous work for the Series 60 ship hull and also more recent discussions between Fuhs and Stern. The calculation methodology consists of an iteration scheme between RANS calculations of the hull flow and lifting surface calculations of propeller forces using the MIT unsteady force program PUF-2.1 [3]. Initially, RANS calculations were performed for the FF1052 hull by the University of Iowa to obtain a non-uniform nominal wake. A harmonic analysis was performed on the calculated nominal wake and an effective wake was determined using the thrust identity wake fraction from propulsion tests. PUF-2.1 calculations were then run for the FF1052 propeller using the calculated effective wake. The PUF-2.1 calculations yielded the unsteady forces on the rotating propeller blades. A post-processor program was written to convert the unsteady forces on the rotating blades calculated by PUF-2.1 into a time-average force at each nonrotating point in the propeller disk.

Originally this post-processor link was to be provided by Fred Stern but when that program could not be found, a new post-processor program was developed. The post-processor program used the thrust coefficient K_T value on each rotating vortex segment to get the K_T value on the corresponding stationary disk element. This was done for each time step and then the time-averaged K_T was calculated at each disk element. It is necessary to normalize the K_T value to account for the difference in area between each PUF-2.1 grid element and the corresponding RANS code grid element, and the pressure jump across the blade can be used for that purpose, so the MIT unsteady force code PUF-3A [4] was modified to print out the pressure jump across each blade element to be used as the input for the post-processor code.

The equations for performing the conversion from rotating blade force to nonrotating disk force are the same as given by Toda et al [2]. The thrust and torque on one blade can be determined by integrating the pressure jump across the blade.

$$K_T(\theta_P) = \frac{1}{\rho n^2 D_P^4} \int_{r_h}^{R_P} \int_{\xi_{TE}}^{\xi_{LE}} f_x(r,\xi,\theta_P) r\, d\xi\, dr \tag{1}$$

$$K_Q(\theta_P) = \frac{1}{\rho n^2 D_P^5} \int_{r_h}^{R_P} \int_{\xi_{TE}}^{\xi_{LE}} f_\theta(r,\xi,\theta_P) r^2\, d\xi\, dr \tag{2}$$

2

where

$$f_x = \Delta p \bar{n} \cdot \bar{e}_x \tag{3}$$
$$f_\theta = \Delta p \bar{n} \cdot \bar{e}_\theta \tag{4}$$

and

$$\xi = \theta - \theta_p \text{ and } \theta_p = 2\pi nt \tag{5}$$
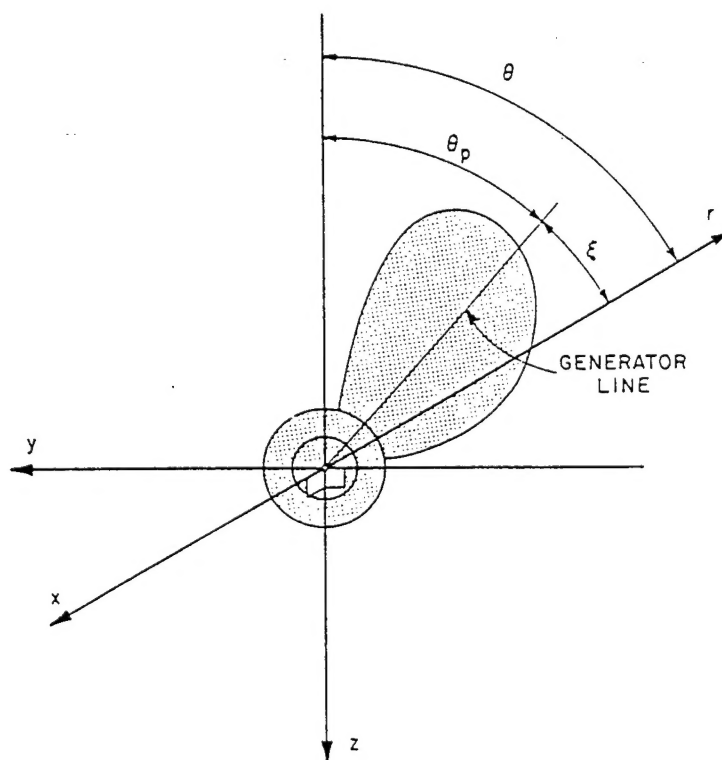
The propeller coordinate system is shown in Fig. 1.

Fig. 1. Propeller coordinate system [2].

The time-average thrust and torque coefficients in the force disk are given as functions of angular position by Toda et al [2] as

$$\overline{K}_T(\theta) = \int_{r_h}^{R_P} \overline{f}_x(r,\theta) r\, dr \tag{6}$$

$$\overline{K}_Q(\theta) = \int_{r_h}^{R_P} \overline{f}_\theta(r,\theta) r^2\, dr \tag{7}$$

where

$$\overline{f}_x = \frac{N}{2\pi\rho n^2 D_P^4} \int_0^{2\pi} f_x\big(r,\theta - \theta_P, \theta_P\big) d\theta_P \tag{8}$$

$$\overline{f}_\theta = \frac{N}{2\pi\rho n^2 D_P^5} \int_0^{2\pi} f_\theta\big(r,\theta - \theta_p, \theta_p\big) d\theta_P \tag{9}$$

This approach appears to be essentially the same as a technique used to calculate helicopter rotor noise. From helicopter theory [5], dipoles on rotating blades are replaced with a disk of stationary dipoles. At each time step, the strength of the stationary dipole is equivalent to the strength of the rotating dipole when enclosed by the blade. Between blades the strength of the stationary dipoles are zero. For the present application, the K_T values on each rotating vortex segment are used to get the K_T on the corresponding stationary disk element. This is done for each time step and then the time average K_T at each disk element is calculated. It was decided that the pressure difference on the rotating vortex segment was needed for the calculations instead of K_T values to account for the differences in size between PUF-2.1 and RANS code grids. Therefore, the MIT unsteady force program PUF-3A was modified to print out the pressure difference on each vortex segment to be used as input for the post-processor code.

Toda found the missing post-processor code for PUF-2.1 and made it available after the present effort was completed. This post-processor converts the unsteady force on the rotating blades calculated by PUF-2.1 to a time-averaged body force in the plane of the propeller. Work has begun on developing another code to convert the time-averaged body force given at PUF-2.1 grid points to body forces at the RANS grid points. The complete calculation procedure is shown as a flowchart in Fig. 2.
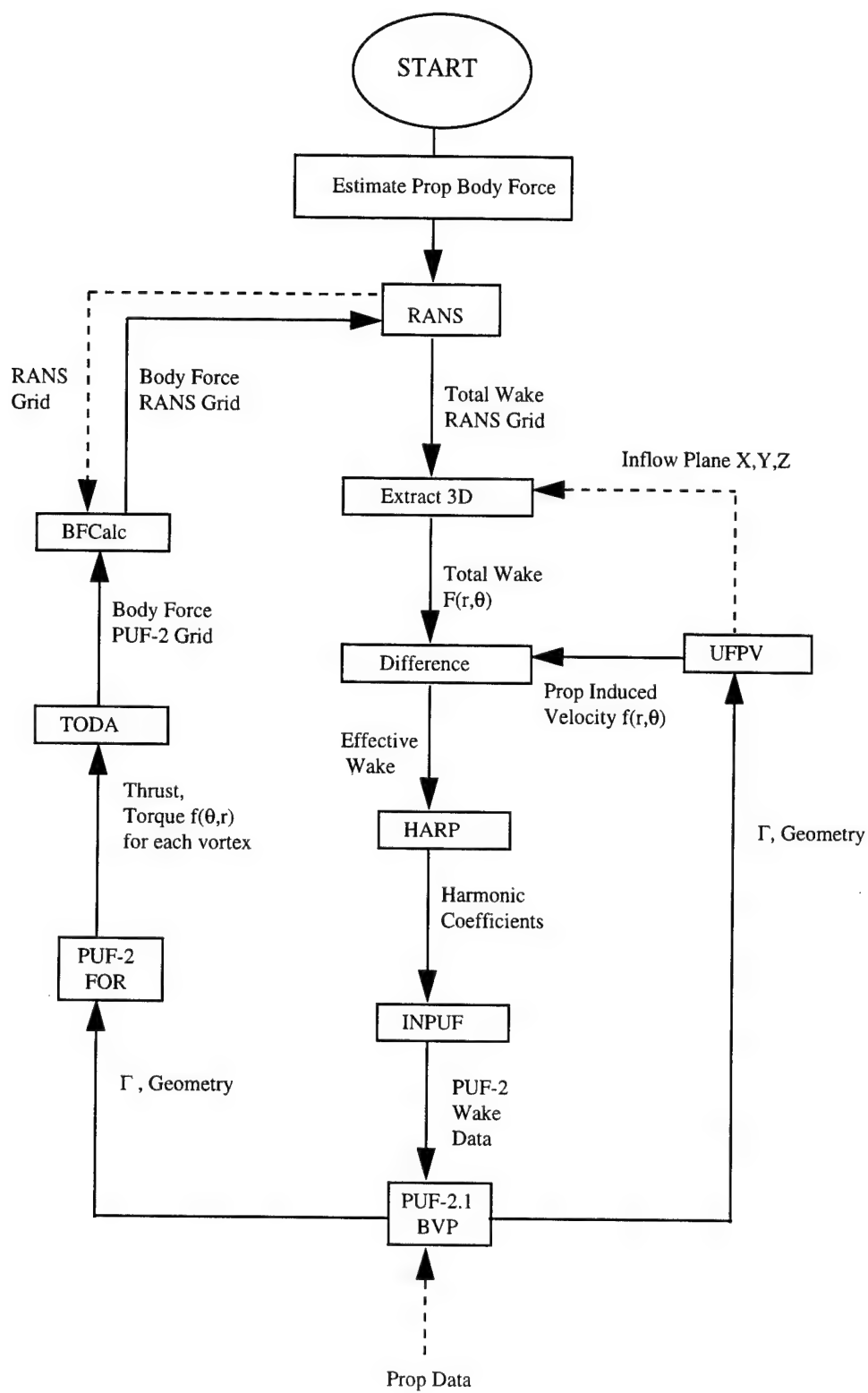
Fig. 2. PUF-2.1/RANS coupling procedure.

ACCOMPLISHMENTS

The work completed this year concentrated on comparing PUF-2.1 and PUF-3A calculations to measurements for test cases and modifying and writing codes to integrate the RANS and unsteady force codes. The PUF-2.1 calculations consisted of calculations for the FF1052 propeller in the open water condition and also the behind the hull condition using the RANS calculated wake. A PUF-2.1 grid sensitivity study was also completed. Modifications were made to the PUF-2.1 and PUF-3A codes to provide the desired force or pressure data in a form that could be used by the post-processor program. A preliminary post-processor program was written.

Calculations were made using PUF-2.1 for the open water condition at various advance coefficients for the FF1052 propeller shown in Fig. 3. The calculated open water thrust and torque coefficients varied from 1 to 8% lower than the measured values. Table 1 and Fig. 4 shows the results of the open water calculations. A sensitivity study was also performed to determine the effect of grid size and time steps per revolution on the open water calculations. The sensitivity study varied the number of spanwise and chordwise vortices on the key blade and in the transition wake. Table 2 shows the different combinations used in the calculations.

The results of the sensitivity study shown in Fig. 5 indicated that there was virtually no variation in the thrust and torque calculations for each of the grids used. The first grid was the grid recommended from the MIT user manual. The number of revolutions were also varied to 4 and 12 but this did not affect the results.

Table 1. Comparison of open water measurements and PUF-2.1 calculations .

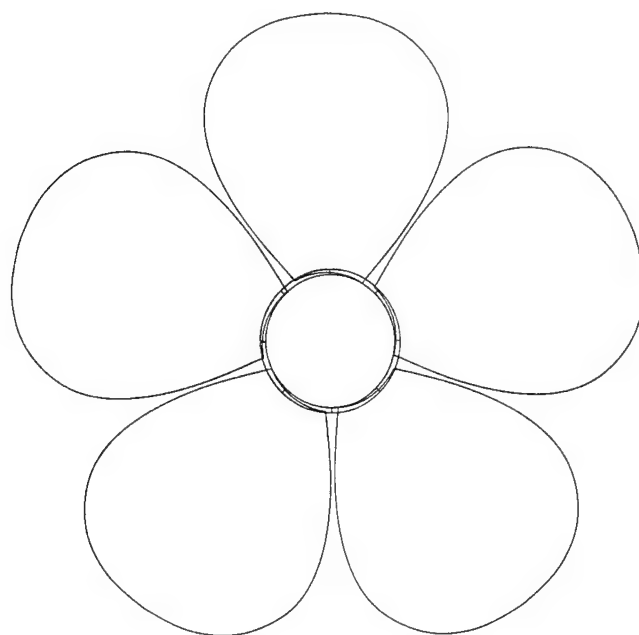| J	KT calc	KT meas	KQ calc	KQ meas
0.2	0.405 (-3.8%)	0.421	0.0610 (-3.3%)	0.0631
0.4	0.320 (-3.0%)	0.330	0.0505 (-1.9%)	0.0515
0.6	0.225 (-5.5)	0.238	0.0380 (-6.8%)	0.0408
0.76	0.150 (-8.0%)	0.163	0.0285 (-7.1%)	0.0307
0.9	0.085 (-8.6%)	0.093	0.0190 (+8.7%)	0.0208

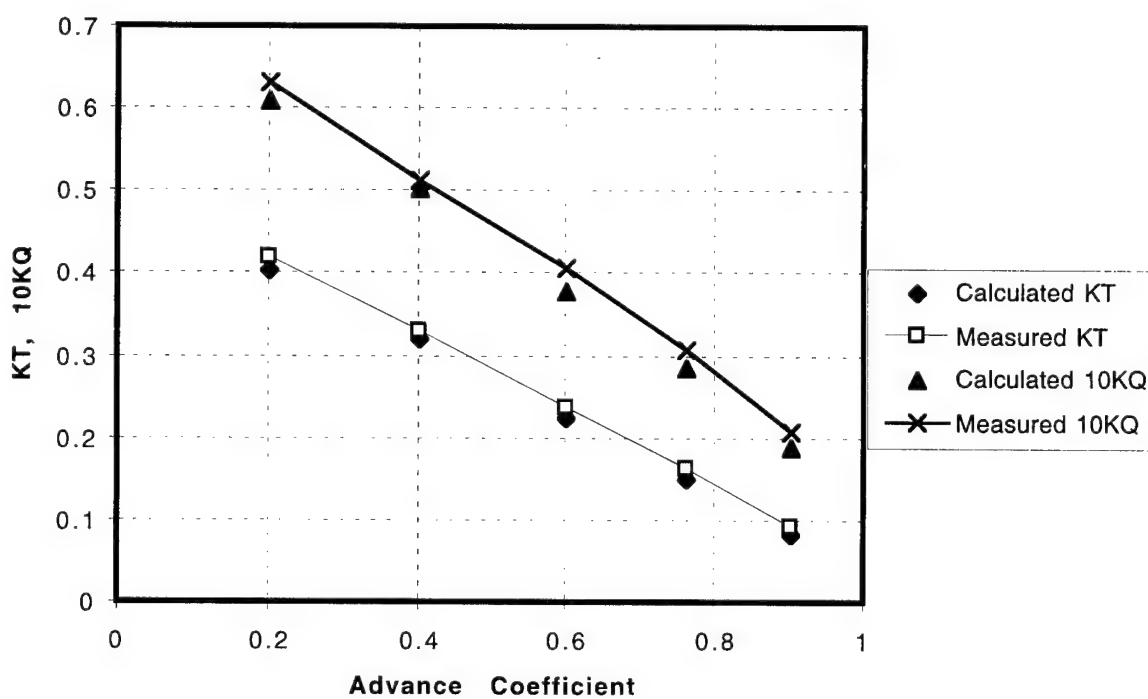Fig. 3. Drawing of FF1052 fleet propeller

Fig. 4. Comparison of measured open water K_T and K_Q to PUF-2.1 calculations.

Table 2. Propeller grid sensitivity study

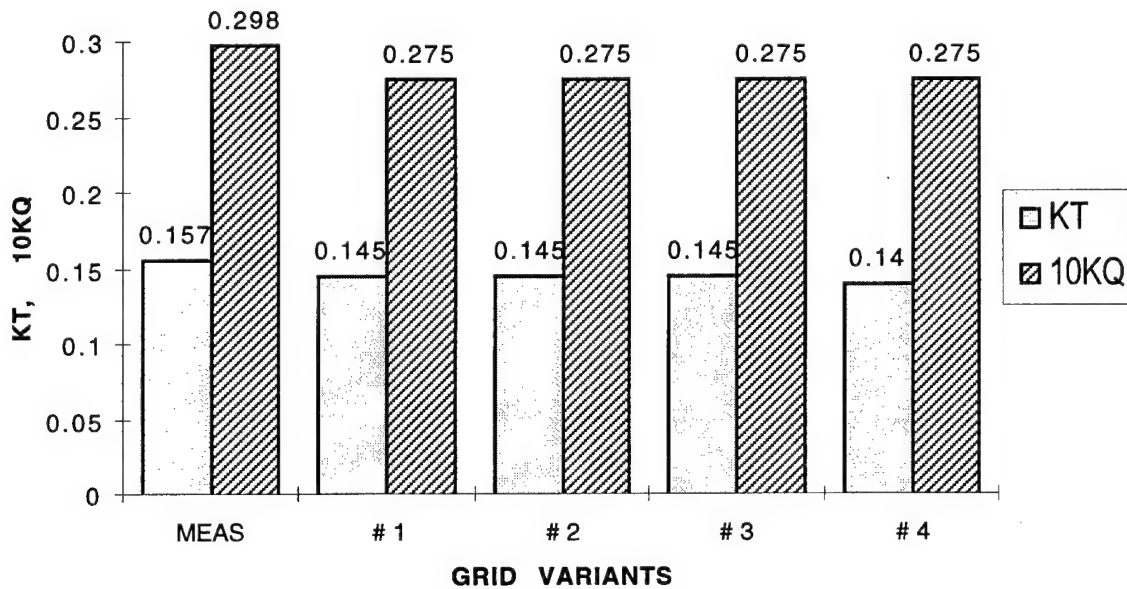|	NUMBER OF VORTICES ON KEY BLADE AND ITS WAKE					
GRID	ACROSS SPAN	ACROSS CHORD	IN TRANS. WAKE	NO. TIME STEPS PER REV.	NO. OF REVS.	NO. TIME STEPS PER BF WAVE
1	9	10	15	60	8	12
2	12	12	15	60	8	12
3	12	12	20	80	8	16
4	15	16	25	100	8	20

Fig. 5. PUF-2.1 grid sensitivity study for open water calculations at J = 0.773.

Calculations were made for the behind hull condition using PUF-2.1 and PUF-3A at the design advance coefficient (J=0.773) for the FF1052 fleet propeller using the calculated nominal wake with the mean axial velocities shifted so that the volume mean wake fraction equals the measured thrust identity wake fraction. The calculated thrust and torque were compared with

powering test measurements. For the PUF-2.1 calculations, a conventional near wake pitch angle β_{nw} is estimated to be the average of the blade pitch angle ϕ and the advance angle β at the tip.

$$\beta_{nw} = (\phi + \beta)/2 \tag{10}$$

The ultimate wake pitch angle β_{uw} is taken to be fifteen percent larger than the near wake pitch angle.

$$\beta_{uw} = 1.15*\beta_{nw}. \tag{11}$$

In Table 3, the PUF-2.1 run designated case A used the conventional wake pitch angles and a drag coefficient of 0.007 as recommended by MIT. The resulting thrust and torque calculations were both lower than the test data. The PUF-2.1 run designated case B attempted to decrease the error between the calculations and the test data by increasing the wake pitch angles by 20%. The resulting thrust calculations corresponded exactly with the measured thrust but the torque calculations were still low by 7.4%. For Case C, PUF-2.1 calculations used the same increased wake pitch angles as case B and a more realistic drag coefficient calculated using the ATTC friction coefficient at the model test Reynolds number and the blade section thickness-to-chord ratio t/c.

$$C_D = 2C_F*[1+1.25(t/c)+125(t/c)^4] = 0.0096. \tag{12}$$

The resulting PUF-2.1 calculations came within 3% of the test data. Calculations using PUF-3A came within 2% of the measured thrust and torque without having to adjust the wake pitch angle or drag coefficient. Some of the differences between calculations and measurements may be due to differences in operating conditions used for the nominal wake calculations and the propulsion test, as shown in Table 4.

Table 3. Comparison of PUF-2.1 and PUF-3A calculations with powering test measurements.

	PUF-2.1 Runs			PUF-3A Run
Powering Test (J=0.7734)	Case A β_{nw}, β_{uw} C_D=0.007	Case B $1.2*\beta_{nw}$, $1.2*\beta_{uw}$ C_D=0.007	Case C $1.2*\beta_{nw}$, $1.2*\beta_{uw}$ C_D=0.0096	
K_T = 0.156	0.145 (-7%)	0.156	0.154 (-1.4%)	0.159 (+2%)
K_Q = 0.0311	0.0275 (-11%)	0.0288 (-7.4%)	0.0303 (-2.7%)	0.0309 (-0.5%)

Table 4. Conditions for nominal wake calculations, wake measurements, and propulsion test measurements.

QUANTITY	MEASURED WAKE	CALCULATED WAKE	PROPULSION TEST
Ship speed (kt)	28.6	27.0	0-30
Displ (tons SW)	4000	4000	4120
Draft (ft)	15.0	15.0	15.2
Appendages	yes*	no	yes

* Wake survey measurements were done with most appendages except for the rudder.

A preliminary post-processor program was written which takes the forces on the key propeller blade calculated from PUF-2.1 or the pressure jump across the blade from PUF-3A at each vortex segment for every time step and interpolates to get the circumferential distribution of K_{Td} on the force disk at each radius for each time step. The circumferential distribution of thrust coefficient on the force disk K_{Td} equals the chordwise distribution of K_T on the blades and equals zero between the blades. Fig. 6 shows the thrust coefficient distribution on the key propeller blade at various time steps, and Fig. 7 shows the thrust coefficient summed over all blades as a function of shaft angle. The circumferential distribution of measured nominal wake at 0.711R is shown in Fig. 8. The nominal wake was measured with and without the downstream dynamometer boat shown in Fig. 9. All calculations were done without the dynamometer boat. In comparing the changes in the force distribution at each time step with the angle of attack of the wake, it is observed that the minimum advance angle which corresponds to the maximum angle of attack occurs at around $\theta_p=270°$ which corresponds to the maximum K_T as it should. Table 5 gives the propeller geometry for the model propeller 4624.

Table 5. Geometry for Propeller 4624

DIAMETER (inches) = 9.224
No. of BLADES   = 5
SCALE RATIO   = 19.515

| r/Ro	PITCH (inches)	RAKE (inches)	SKEW (deg)	CHORD (inches)	CAMBER (inches)	THICKNESS (inches)
.217	10.443	.000	.000	2.103	.044	.367
.250	10.370	.000	.000	2.277	.052	.343
.300	10.259	.000	.000	2.525	.063	.310
.400	10.038	.000	.000	2.985	.080	.251
.500	9.809	.000	.000	3.387	.088	.200
.600	9.564	.000	.000	3.714	.086	.156
.700	9.299	.000	.000	3.922	.073	.116
.800	8.965	.000	.000	3.889	.054	.082
.900	8.487	.000	.000	3.331	.030	.053
.925	8.344	.000	.000	3.057	.023	.048
.950	8.182	.000	.000	2.681	.016	.043
.960	8.115	.000	.000	2.478	.013	.042
.970	8.045	.000	.000	2.226	.009	.041
.980	7.973	.000	.000	1.901	.006	.039
.990	7.896	.000	.000	1.455	.003	.038
.995	7.857	.000	.000	1.000	.002	.037
1.000	7.818	.000	.000	0.268	.000	.037
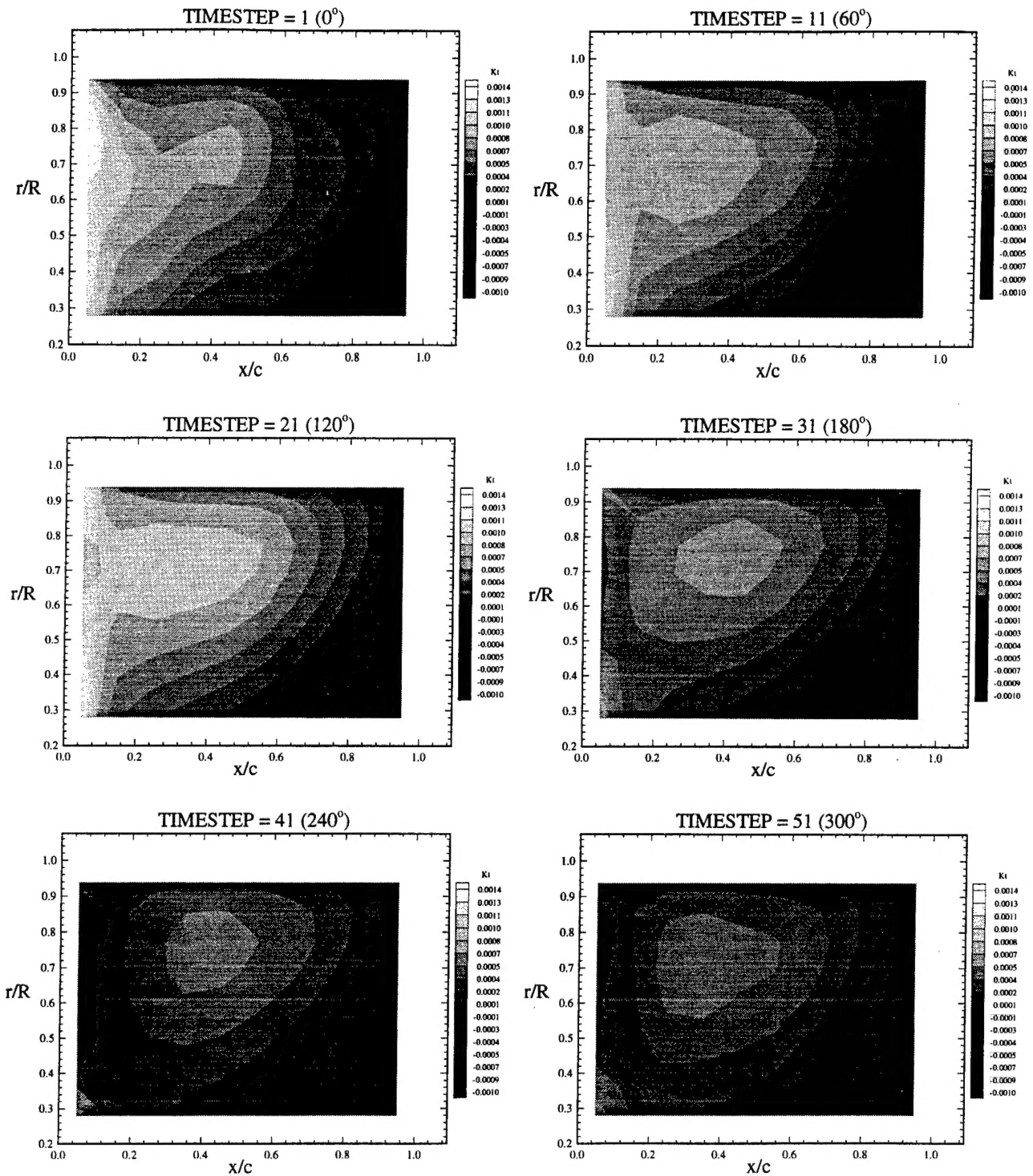
Fig. 6. PUF-2.1 thrust coefficient on key blade at various time steps.
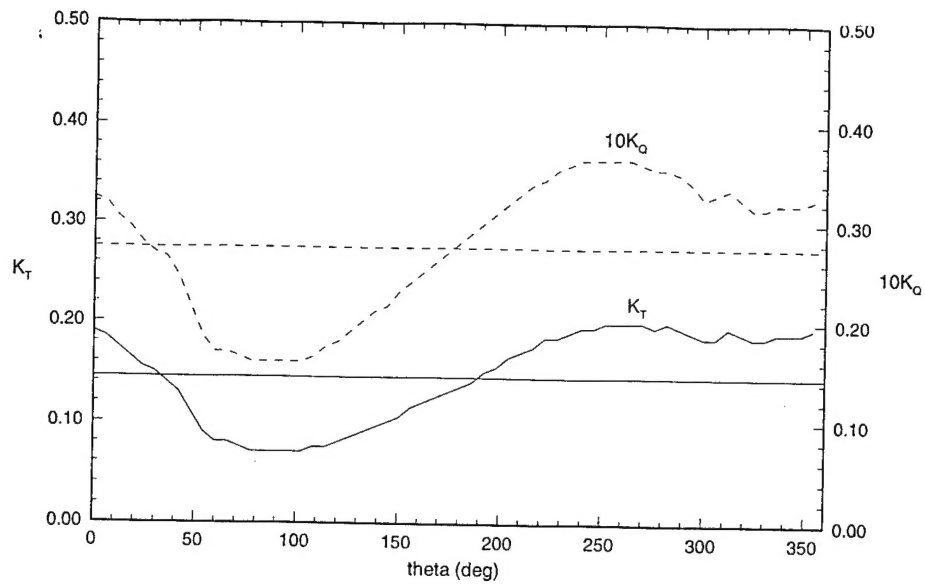
Fig. 7. PUF-2.1 thrust and torque coefficients integrated across blade as function of shaft angle, using first 16 harmonics of measured wake.
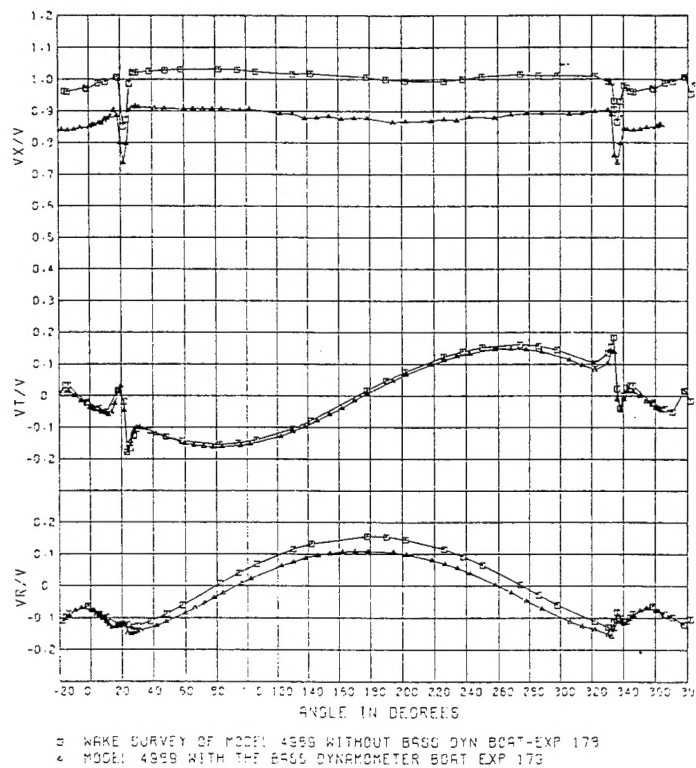

Fig. 8. Nominal velocities measured at 0.711R with and without the Bass dynamometer boat.
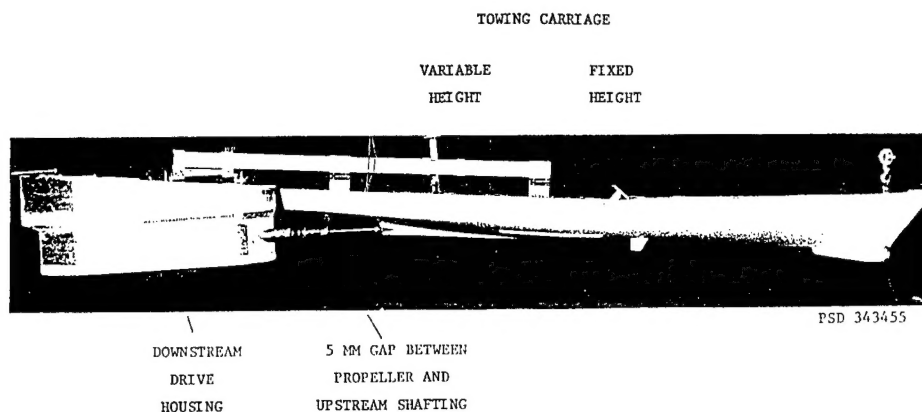
13

TOWING CARRIAGE

VARIABLE   FIXED
HEIGHT   HEIGHT

PSD 343455

DOWNSTREAM   5 MM GAP BETWEEN
DRIVE   PROPELLER AND
HOUSING   UPSTREAM SHAFTING

Fig. 9. Experimental arrangement for wake surveys showing Bass dynamometer boat.

PLANS AND TRANSITION POTENTIAL

The work done this year is the start of a ten year 6.1 basic research plan. The goal for the first three years is to develop and validate the calculation method for simple unappended configurations. The method is based on non-uniform time-average propeller forces calculated using a lifting surface method. The five year goal includes automation of the gridding of appendages as well as the hull and propulsor, and validation of the method for appended hull configurations. The ten year goal is to have an integrated code that can be used as a design tool for complete hull/propulsor/appendage systems. By the completion of the ten year period a method for solving the hull flow at each propeller time step is desired and ultimately unsteady RANS codes will be used to calculate the entire flow.

The basic research planned can be readily transitioned to 6.2 applied research. The coupling method that is being developed could be applied to most 3-D RANS codes. The prediction capabilities that could be developed using this new method include far wake signatures, propeller inflow for new hull and appendage configurations, propeller mean thrust and torque and unsteady bearing forces, propeller-induced hull surface forces (mean and unsteady) and maneuvering forces.

14

ACKNOWLEDGMENTS

REFERENCES

1.	Stern, F., et al, "Computation of Viscous Flow Around Propeller-Body Configurations: Series 60 CB=0.6 Ship Model", SNAME Journal of Ship Research, Vol. 38, No. 2, pp. 137-157 (June 1994).

2	Toda, Y., et al, "Mean Flow Measurements in the Boundary Layer and Wake of a Series 60 CB=0.6 Model Ship With and Without Propeller." SNAME Journal of Ship Research, Vol. 34, No. 4, pp. 225-252 (Dec 1990).

3.	Kerwin, J.E., and C.S. Lee, "Prediction of Steady and Unsteady Marine Propeller Performance by Numerical Lifting-Surface Theory", SNAME Transactions, Vol. 86, pp. 218-253 (1978).

4.	Kinnas, S.A., "A Numerical Method for the Analysis of Cavitating Propellers in a Non-uniform Flow, MIT-PUF-3 Program Documentation", Massachusetts Institute of Technology Department of Ocean Engineering Report 83-7, June 1983.

5.	Johnson, W., Helicopter Theory, Dover Publications, New York NY (1980).